Electronic Supplementary Material (ESI) for Green Chemistry.

Supporting Information for: Selective Adsorption of Rare Earth Elements onto Functionalized Silica Particles

Jonathan C. Callura,[a] Kedar M. Perkins,[b] Clinton W. Noack,[a] Newell R. Washburn,[b] David A. Dzombak,[a] and Athanasios K. Karamalidis*[a]

Carnegie Mellon University, Pittsburgh, Pennsylvania 15213, USA

[a]*Department of Civil and Environmental Engineering*

[b]*Department of Chemistry*

**Corresponding Author*

E-mail: akaramal@andrew.cmu.edu

This document contains 5 tables and 6 figures

Table S1. Approximate average reported concentrations of selected cations in geothermal brines (mg/L).

Study	# Samples	Na^+	Ca^{2+}	Mg^{2+}	Al^{3+}	Fe^{2+}	Zn^{2+}
Nicholson (1993)[1]	N.R.	<2,000	<50	<0.1	<2	<1	N.R.
Clark et al. (2010)[2]	>1,887	1,600	200	70	10	20	10
Gallup (1998)[3]	>8	18,000	6,500	150	1	850	300
Maimoni (1982)[4]	5	42,000	18,000	100	<1	200	150

N.R. = Not Reported

Table S2. Standard instrument settings for Agilent 7700x ICP-MS measurements. Oxygen-free grade argon was used as the carrier and dilution gas. Ultra high-purity helium was used in the reaction cell. Tuning solutions purchased from Agilent were diluted 1000:1. Table adapted from Noack, et al. (2016).

	Parameter	Value
Plasma	RF power	1600 W
	Nebulizer pump rate	0.10 rps
	Carrier argon flow rate	0.61 L/min
	Dilution argon flow rate	0.36 L/min
Lenses	Extract 1	0.0 V
	Extract 2	-200.0 V
	Omega bias	-110 V
	Omega lens	9.6 V
	Cell entrance	-110 V
	Cell exit	-150 V
	Deflect	-74.8 V
	Plate bias	-150 V
Octopole reaction cell	Octopole bias	-100.0 V
	Octopole RF	200 V
	He flow rate	10 mL/min
	Energy discrimination	7.0 V
Data acquisition	Replicates	5
	Integration time	0.3 s
Masses monitored	^{145}Nd, ^{157}Gd, ^{165}Ho	
Oxides and doubly charged	$^{140}Ce^{16}O^+/^{140}Ce$	< 2.1%
	$^{140}Ce^{2+}/^{140}Ce$	< 1.6%

Table S3. Elemental composition of Great Salt Lake brine. Data provided by the Idaho National Laboratory (sampling location: 40.735287, -112.212512).

Parameter	Unit	Natural C
pH	-	7.92
Temp. (Field)	^{o}C	1.8
Alkalinity	mg as $CaCO_3$	446
Dissolved O	mg/L	2.7
F	mg/L	<10
Cl	mg/L	85,682
SO_4	mg/L	10,358
Br	mg/L	51.2
NO_3	mg/L	<10
Li	mg/L	24
Be	mg/L	0.0352
Na	mg/L	51,330
Mg	mg/L	5,169
Al	mg/L	0.328
K	mg/L	4,101
Ca	mg/L	323
SiO_2(aq)	mg/L	27.8
Ga	mg/L	0.0342
As	mg/L	0.206
Se	mg/L	0.213
Rb	mg/L	4.355
Sr	mg/L	3.23
In	mg/L	0.0336
Cs	mg/L	0.0538
Ba	mg/L	0.168
Bi	mg/L	0.0419

Parameter	Unit	Natural C	Spiked	Total C
Sc	ug/L	7.15E-03	55.56	55.56
Y	ug/L	9.64E-02	55.56	55.65
La	ug/L	1.60E-01	55.56	55.72
Ce	ug/L	2.02E-01	55.56	55.76
Pr	ug/L	3.99E-02	55.56	55.60
Nd	ug/L	1.56E-01	55.56	55.71
Sm	ug/L	3.07E-02	55.56	55.59
Eu	ug/L	6.21E-03	55.56	55.56
Gd	ug/L	3.36E-02	55.56	55.59
Tb	ug/L	4.00E-03	55.56	55.56
Dy	ug/L	1.90E-02	55.56	55.57
Ho	ug/L	3.71E-03	55.56	55.56
Er	ug/L	9.83E-03	55.56	55.57
Tm	ug/L	1.60E-03	55.56	55.56
Yb	ug/L	9.08E-03	55.56	55.56
Lu	ug/L	1.73E-03	55.56	55.56
Th	ug/L	1.32E-02	55.56	55.57
U	ug/L	1.17E+01	55.56	67.23

Table S4. Separation factors for REE/U from experiments performed in Great Salt Lake brines. Higher values are shaded in blue.

Solid	pH	Separation Factors ($\alpha_{REE/U}$)															
		Sc	**Y**	**La**	**Ce**	**Pr**	**Nd**	**Sm**	**Eu**	**Gd**	**Tb**	**Dy**	**Ho**	**Er**	**Tm**	**Yb**	**Lu**
Raw Silica	2.63	1.9	0.0	0.0	0.0	0.1	0.0	0.1	0.2	0.0	0.3	0.4	0.3	0.3	0.3	0.2	0.3
	6.91	0.1	0.0	0.0	0.0	0.0	0.0	0.0	0.0	0.0	0.0	0.0	0.0	0.0	0.1	0.1	0.2
	7.77	0.1	0.2	0.0	0.1	0.1	0.1	0.1	0.1	0.1	0.2	0.2	0.3	0.3	0.4	0.6	0.5
Aminated Silica	6.14	0.0	0.0	0.0	0.0	0.0	0.0	0.0	0.0	0.0	0.0	0.0	0.0	0.0	0.0	0.0	0.0
	8.42	2.8	0.5	0.0	0.3	0.1	0.1	0.2	0.2	0.2	0.4	0.5	0.6	0.7	0.9	1.7	1.3
	8.99	1.9	0.7	0.4	0.5	0.5	0.5	0.5	0.5	0.5	0.7	0.7	0.8	0.9	0.9	1.4	1.1
TD-DTPADA	2.31	24.3	58.6	51.7	136.6	200.1	155.1	141.4	101.0	110.0	104.0	102.5	98.7	104.5	104.6	113.6	115.6
	2.34	24.2	59.7	65.6	170.5	204.8	128.3	125.7	98.0	116.5	104.9	93.8	96.1	98.5	101.3	110.3	110.0
	2.37	30.3	77.4	53.6	147.9	220.9	210.3	182.1	129.5	157.9	141.9	131.3	138.4	135.1	145.7	147.0	154.2
	2.45	29.5	81.4	18.0	47.6	108.3	94.1	244.3	178.5	177.3	204.7	203.3	191.1	166.2	210.7	204.8	185.1
	2.48	27.9	72.5	15.2	42.1	97.6	131.9	218.3	164.8	162.1	192.1	178.0	184.6	183.3	182.0	184.4	173.0
	2.50	32.2	77.3	17.4	42.7	107.7	142.8	225.2	173.6	169.3	204.1	193.7	197.7	194.1	196.4	206.8	181.9
	2.68	4.0	24.4	9.0	19.4	34.8	37.2	37.0	29.7	27.2	25.5	22.8	22.4	24.4	26.2	33.0	29.0
	2.72	5.1	24.1	7.8	17.3	31.4	38.2	38.8	31.4	28.8	27.3	25.1	24.7	25.2	28.1	37.8	30.2
	7.08	1.5	0.5	0.5	0.4	0.4	0.4	0.3	0.3	0.3	0.3	0.3	0.4	0.4	0.5	0.6	0.6
	7.21	1.6	0.2	0.3	0.2	0.2	0.2	0.2	0.2	0.2	0.2	0.2	0.2	0.2	0.3	0.3	0.3
	8.22	4.4	0.7	0.7	0.7	0.5	0.5	0.5	0.5	0.5	0.5	0.5	0.6	0.7	0.8	1.0	1.1
	8.33	2.2	0.5	0.4	0.5	0.4	0.4	0.4	0.3	0.4	0.4	0.4	0.4	0.5	0.5	0.6	0.7

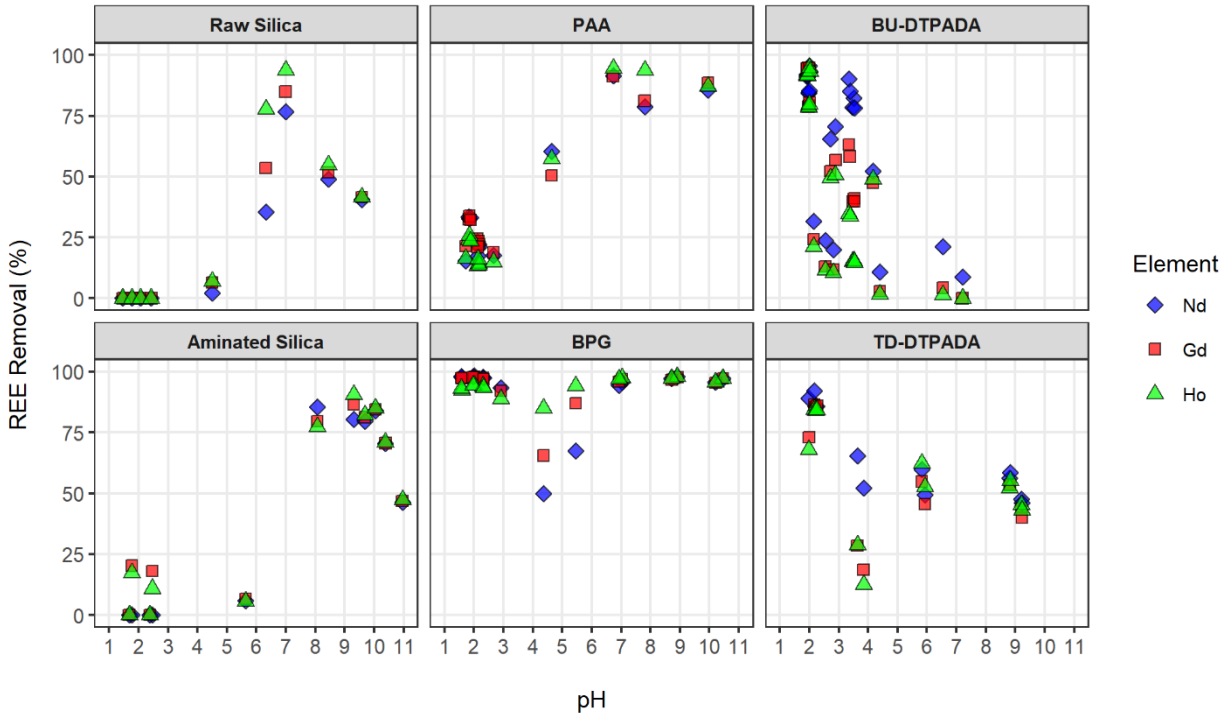

Figure S1. Full pH edge adsorption dataset for 100 µg/L mixtures of Nd, Gd, and Ho in 0.5M NaCl. Adsorption reactions were performed for 3 hours at T = 20°C, using adsorbent loadings of 10 g/L.

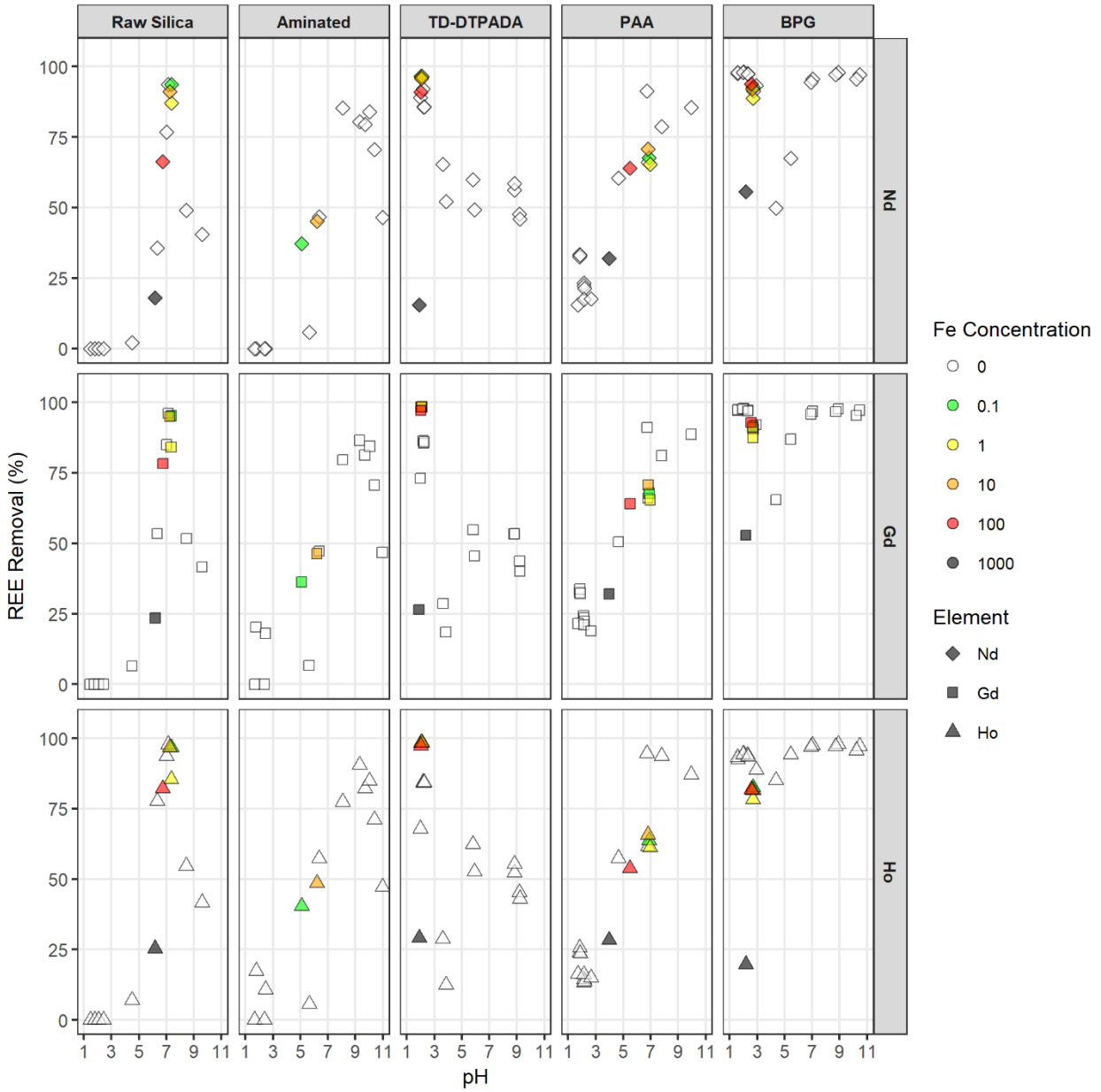

Figure S2. Adsorption pH trends for 100 µg/L mixtures of Nd, Gd, and Ho in 0.5M NaCl with and without iron. Iron concentrations are denoted by the color of the data points. A single pH value was targeted for each solid for all samples containing Fe, though high concentrations of iron lead to decreased equilibrium pH. Adsorption reactions were performed for 3 hours at T = 20°C, using adsorbent loadings of 10 g/L.

Elution trends for BPG were similar to the TD-DTPADA, with a plateau in recovery observed above 1N (Figure S3). Overall REE recovery rates upon elution were relatively low for BPG (maximum of 60% recovered). It is hypothesized that this decrease in elution efficiency may be attributable to residual reactants from the functionalization process, i.e., excess BPG molecules not covalently bound to the silica support surface remaining on the fresh BPG particle surfaces during the uptake step. These weakly attached compounds would be washed away prior to the elution, carrying with them some complexed REE and thus causing discrepancies between the calculated adsorbed mass and the measured concentrations in elution samples. Subsequent use cycles yielded improved performance and REE recovery, as discussed and shown in Figure 7 of the main text.

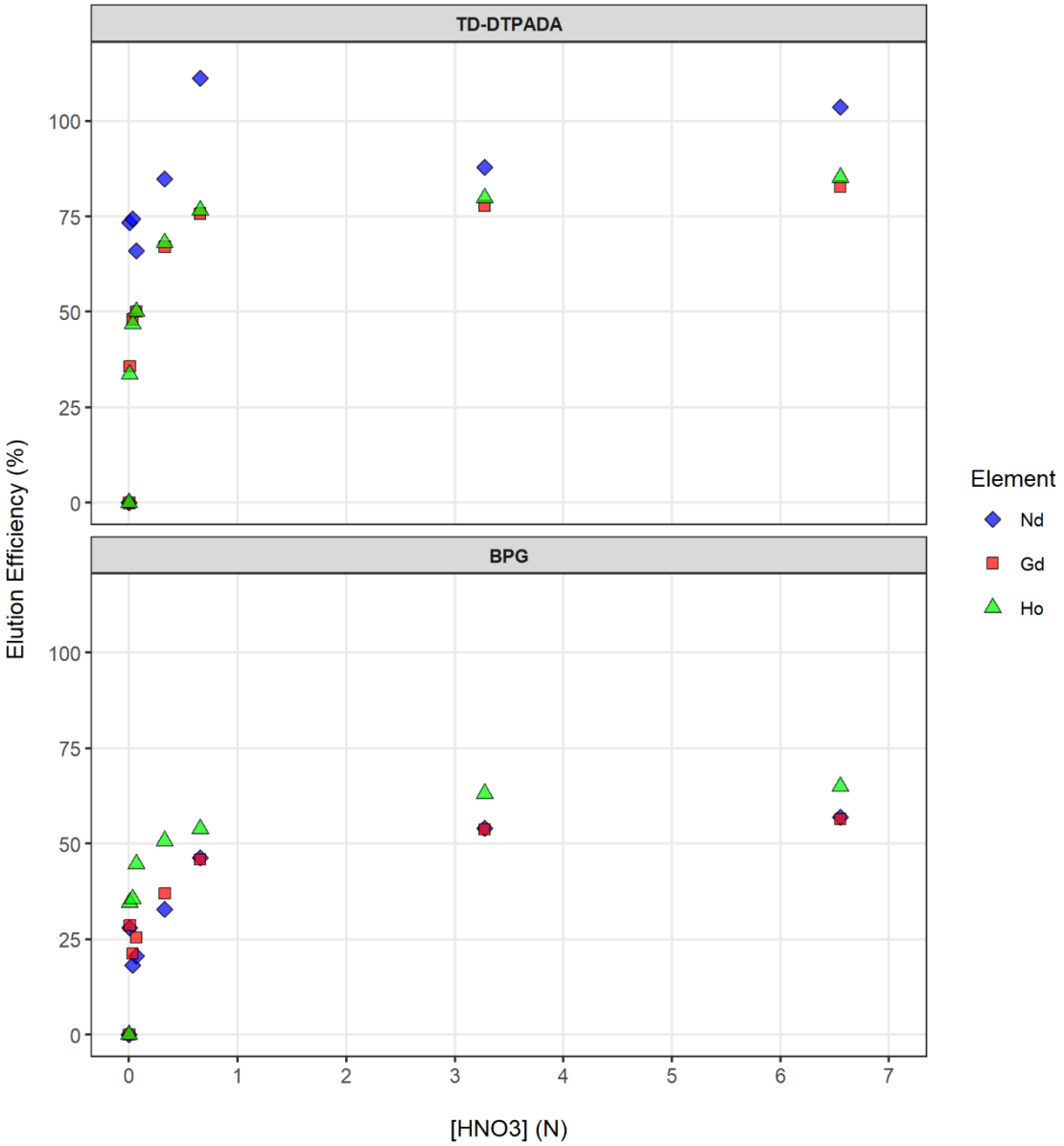

Figure S3. REE elution efficiency for DTPADA and BPG on silica as a function of nitric acid strength after one use cycle. Adsorption cycles were performed at pH ~1.8.

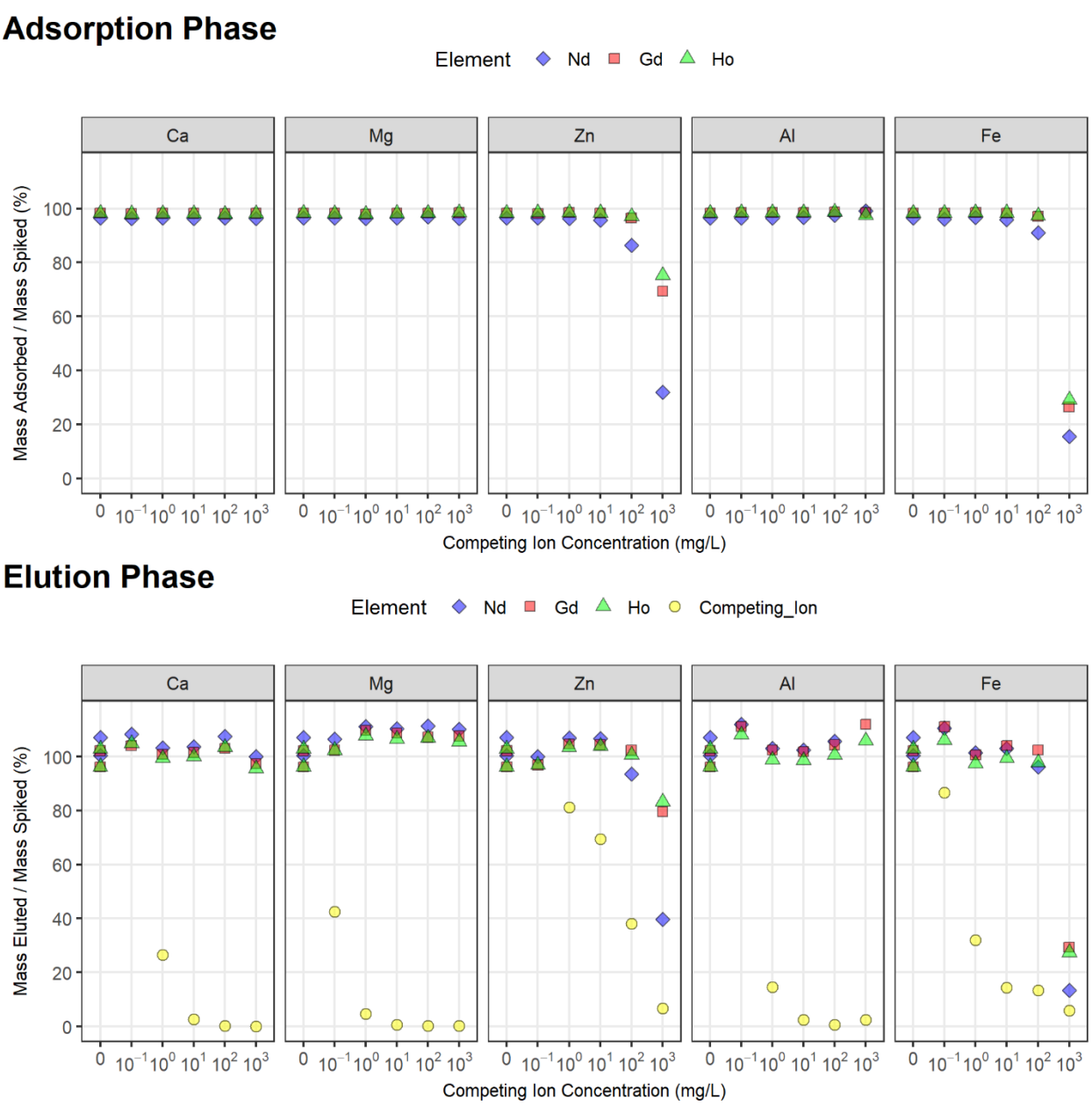

Figure S4. Ratio of mass eluted to mass spiked for each element eluted from TD-DTPADA particles after the competitive adsorption study. Adsorption was conducted at pH ~ 2 and room temperature.

After completion of adsorption reactions for the competition study (10g/L adsorbents in 0.5M NaCl containing 100ppb of each REE + varied concentrations of competing ions), TD-DTPADA adsorbents were separated from solution, rinsed with deionized water, dried overnight, then adsorbed elements were eluted using 0.75N HNO_3. The elution data shown in Figure S4 confirm the adsorption phase results from Figure 3B of the main text. The low ratio of mass eluted to mass spiked indicates inefficient adsorption of competing ions, particularly in higher concentration ranges, whereas REE uptake was approximately 100% in nearly all samples.

This data is summarized in Figure S5, which shows the average enrichment factor for each REE relative to the competing ion as a function of molar ratios for spiked concentrations of the competing ions over each REE. Here, the REE enrichment factors and molar ratios are defined by the following equations, where C_{elu} = eluted concentration and C_i = initial spiked solution phase concentration. Larger enrichment values may be interpreted as more efficient REE separation at a given molar ratio.

$$REE\ Enrichment\ Factor = \frac{[{}^{C_{elu}}/_{C_i}]_{REE}}{[{}^{C_{elu}}/_{C_i}]_{Competing\_Ion}}$$

$$Spiked\ Adsorbate\ Molar\ Ratio = \frac{C_{i,Competing\_Ion}}{C_{i,REE}}$$

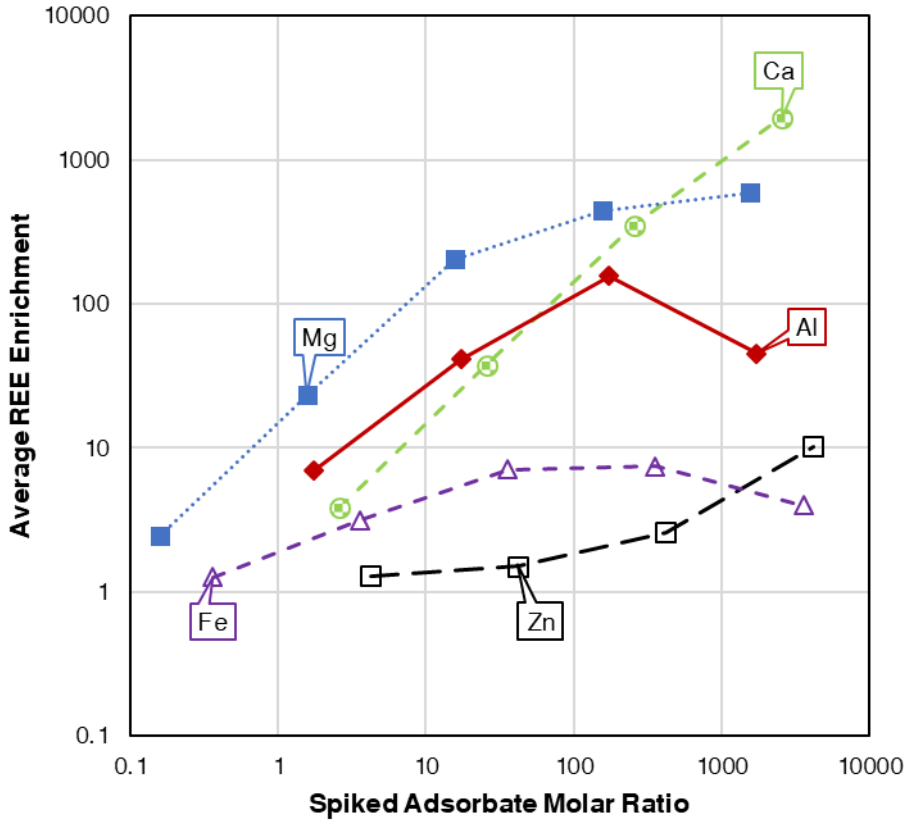

Figure S5. Enrichment factors for REE relative to competing ions shown as a function of molar ratios of spiked adsorbate concentrations (adsorbent = TD-DTPADA).

In addition to the binary system study (i.e. REE + 1 competing ion), a competitive isotherm study was conducted to assess the selectivity of the TD-DTPADA functionalized adsorbents for lanthanides in the presence of multiple competing ions. Samples were prepared by mixing equal concentrations of 10 elements (3 REE + 7 competing ions) in a 0.5M NaCl solution with 10g/L of functionalized adsorbents. Several of the higher spiked concentrations were beyond the range of expected site saturation (i.e. sorbate concentrations exceeded the available binding sites on the adsorbents). Samples were reacted until equilibrium was reached, then the solution phase was sampled and analyzed to determine concentrations of each analyte. Results from this experiment are presented in Figure S6 and show a high degree of selectivity for the lanthanides over other metals, though Zn and Cu also appeared to bind to a lesser degree. Differences between spiked and equilibrium concentrations for Al were too small to detect, so the Al trends are not shown on this plot. The trends observed here agree with those from Figure S4 and Figure 3 of the main text: Ca, Mg, and Al do not inhibit adsorption of REE to the TD-DTPADA adsorbents.

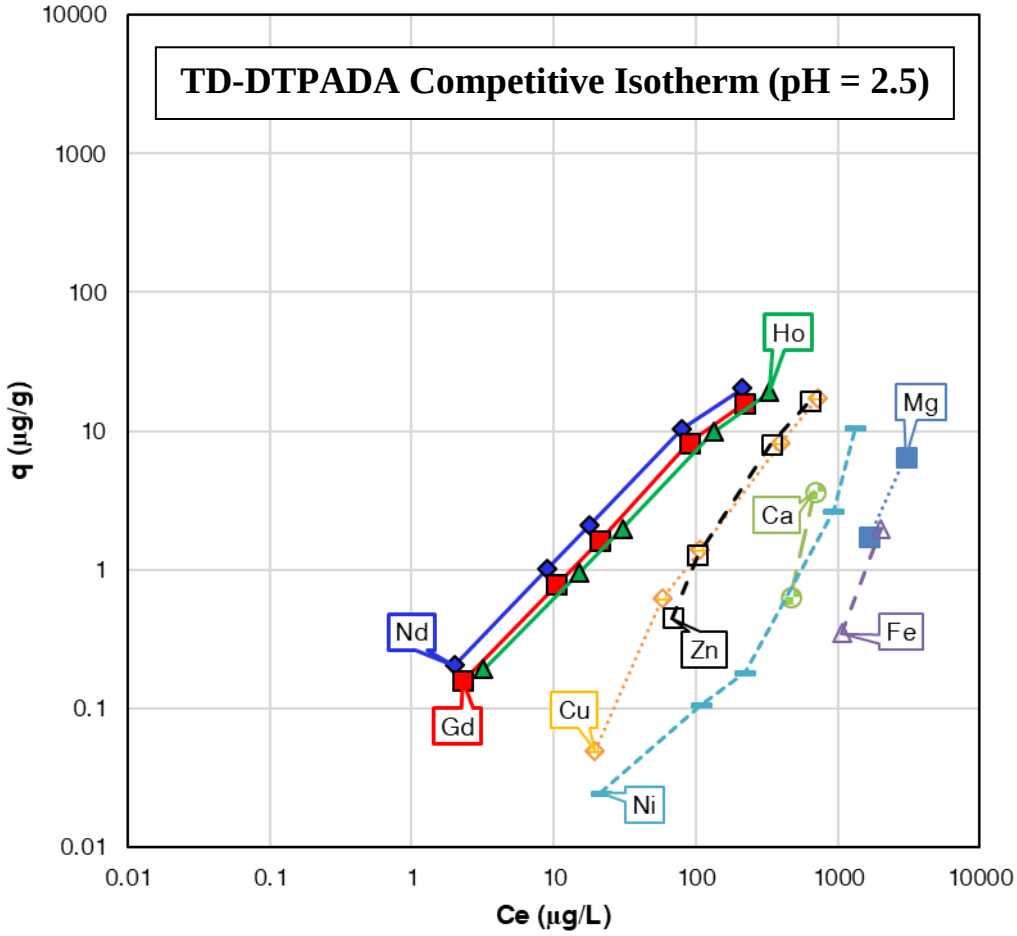

Figure S6. Competitive isotherm results TD-DTPADA functionalized adsorbents with a mixture of 10 elements (7 competing ions and 3 REE) spiked at equal concentrations in a 0.5M NaCl solution. Equilibrium solution-phase concentrations are shown on the x-axis, while the y-axis shows adsorbed concentrations for each element (pH = 2.5, T ~ 20°C, adsorbent loading = 10g/L).

After completion of the competitive isotherm study, the sorbents were separated from solution, rinsed with DI water, and dried overnight. Next, the adsorbed metals were eluted from the particle surfaces using 0.75N HNO_3. Recovery efficiencies (Mass Eluted / Mass Spiked) were calculated for each element based on the measurements taken on the elution, and separation factors were determined using methods previously discussed. These results are presented in Table S5. Separation factors > 1 indicate that TD-DTPADA adsorbents exhibited a high degree of selectivity towards REE compared to the other elements present in solution.

Table S5. Separation factors for REE over each competing ion from the competitive isotherm study using TD-DTPADA. These results are based on recovery for each element upon elution from the adsorbents.

Average C-spiked (mg/L)	**Average Separation Factor ($\alpha_{REE/Competing\_Ion}$)**						
	Mg	**Al**	**Ca**	**Fe**	**Ni**	**Cu**	**Zn**
0.02	76.8	44.5	199.3	36.1	15.9	9.5	12.9
0.11	35.1	16.5	41.5	14.0	40.2	12.3	5.0
0.23	38.2	11.8	20.4	20.5	46.6	12.3	4.1
1.15	154.7	42.1	71.8	40.4	32.9	11.0	4.0
2.29	194.4	57.6	71.1	33.0	10.2	6.8	2.9

References

(1) Nicholson, K. Water Chemistry. In *Geothermal Fluids: Chemistry and Exploration Techniques*; Springer Berlin Heidelberg: Berlin, Heidelberg, 1993; pp 19–85.

(2) Clark, C. E.; Harto, C. B.; Sullivan, J. L.; Wang, M. Q. Water Use in the Development and Operation of Geothermal Power Plants. **2010**.

(3) Gallup, D. L. Geochemistry of geothermal fluids and well scales, and potential for mineral recovery. *Ore Geol. Rev.* **1998**, *12* (4), 225–236.

(4) Maimoni, A. Minerals recovery from salton sea geothermal brines: a literature review and proposed cementation process. *Geothermics* **1982**, *11* (4), 239–258.